Monte Carlo simulations of chemical reactions on a surface with time-dependent reaction-rate constants

ELSEVIER

Computer Physics Communications 86 (1995) 1–12

Computer Physics Communications

Monte Carlo simulations of chemical reactions on a surface with time-dependent reaction-rate constants

A.P.J. Jansen [1]

Laboratory for Inorganic Chemistry and Catalysis, Eindhoven University of Technology, P.O. Box 513, 5600 MB Eindhoven, The Netherlands

Received 22 August 1994; revised 12 October 1994

Abstract

We present Monte Carlo methods with a correct real-time dependence for simulating chemical reactions on a surface that have reaction-rate constants that may vary in time. Explicit expressions are derived for the simulation of temperature-programmed desorption experiments, where temperature is a linear function of time. Using the first-reaction method it is shown that the computational time per reaction scales only as the logarithm of the linear dimension of the surface.

1. Introduction

Temperature-programmed desorption (TPD) is a standard technique for studying adsorbates on a surface. First, atoms or molecules are adsorbed on the surface at low temperature. Then the temperature is increased, and the desorbing chemical species are monitored. By analysing the desorption rate as a function of temperature valuable information can be obtained such as adsorption energies, the number and nature of the adsorption sites, reaction mechanisms, interactions between adsorbates, etc. [1,2]. However, it is in general not easy to extract from TPD spectra quantitative data like activation energies and pre-exponential factors of reactions. In most analyses macroscopic reaction-rate equations of chemical kinetics based on the mean-field approximation are used. These analyses are often complicated by factors like surface heterogenity [3], lateral adsorbate–adsorbate interactions [3–8], and islanding [9,10]. To avoid the shortcomings of the mean-field approximation Monte Carlo (MC) methods have been used in which the local environment of an adsorbate molecule is explicitly included. (For these and other methods used for analysing TPD spectra see Refs. [11] and [12].) Fascinating subjects such as kinetic phase transitions [13], and chemical oscillations [14,15] have been studied with these MC methods. With respect to TPD experiments MC has deepened our insight, however, again only qualitatively. Quantitative data have hardly been obtained, because in most MC algorithms the time dependence is not described properly; i.e., some MC time is used.

Two MC methods for chemical reactions with good time dependence have been described by Gillespie [16,17]. For simulating TPD experiments, however, there are two reasons why these methods have to be adapted. First, Gillespie has dealt with homogeneous systems. As mentioned above this is a too crude approximation for our systems. It is obvious how to formulate his methods for heterogeneous systems though [18,19]. Second, Gillespie has dealt with reactions at a fixed temperature. The main subject of this pa-

[1] E-mail address: tgtatj@chem.tue.nl

SSDI 0010-4655(94)00155-3

per is the extension of Gillespie's methods to time-dependent reaction-rate constants. Although we are primarily interested in simulating TPD, the methods that we will discuss can also be used for other processes than desorption; e.g., catalytic reactions with a variable feed [20].

The contents of this paper are as follows. Section 2 starts with a description of the model of the system and a master equation for the reactions. The important point is that the transition probabilities in this equation will be time dependent. This necessitates a rederivation of the MC method to solve the master equation. The theory is given for an arbitrary time dependence of the transition probabilities, but in Section. 2.3 some analytical results will be given for the usual linear time dependence of the temperature in TPD experiments. Three MC methods will be described; two of them being similar to those of Gillespie. We will argue that for surfaces another method is the most efficient than in Gillespie's case. Section 3 discusses four examples. We show that our MC method gives the same results as macroscopic chemical kinetics when the mean-field approximation is valid. Section 4 summarises the most important aspects of this paper.

2. Theory

2.1. Modelling the system and the reactions

We model the surface as a collection of sites, each possibly occupied by an adsorbate. In the actual simulation we will use a regular grid and periodic boundary conditions. However, such restrictions are not used in this section. We will indicate a particular configuration of the surface by lower case Greek letters $(\alpha, \beta, \ldots)$. A stochastic description of the system is obtained by using probability $\mathcal{P}_\alpha$, which is the probability of having the system in configuration α. The way in which the probabilities for all possible configurations change with time is described by a master equation.

$$\frac{\mathrm{d}\mathcal{P}_\alpha}{\mathrm{d}t} = \sum_\beta \left[W_{\alpha\beta}\mathcal{P}_\beta - W_{\beta\alpha}\mathcal{P}_\alpha\right]. \tag{1}$$

The summation is over all possible configurations, but we define $W_{\alpha\alpha} = 0$. The first term describes the changes leading to configuration α, and the second term those that can occur in configuration α [21]. A change of configuration is nothing but a reaction. As we will see, the transition probabilities per unit time $W_{\alpha\beta}$ are closely related to the reaction-rate constants from macroscopic chemical kinetics.

The master equation, and in particular the transition probabilities, can be obtained either from first principles or empirically. First, Eq. (1) can be derived from the Liouville equation by partitioning the configuration space of the system in such a way that each configuration α corresponds to a region, or a number of regions, in configuration space. Such a derivation is quite similar to the derivation of the expression for the reaction rate constant in variational transition state theory [22]. In this way it is possible to calculate the transition probabilities $W_{\alpha\beta}$ using, for example, quantum-chemical methods [23–25]. It also implies that time in Eq. (1) is real time. Second, it is possible to derive the macroscopic reaction-rate equations from the master equation. This yields relations between the transition probabilities $W_{\alpha\beta}$ and macroscopic rate constants. In this way the transition probabilities $W_{\alpha\beta}$ can be obtained from experiments. Examples of such derivations will be given in Section 3.

2.2. Monte Carlo methods for solving the master equation

The master equation can only be solved analytically for some simple cases. Because of the large number of configurations, it is not even possible to get solutions for the probabilities $\mathcal{P}_\alpha$ numerically. However, using MC methods information can be obtained about the reactions on a surface that are described by Eq. (1). We will discuss three of these methods in some detail, and compare their efficiency.

The simplest method is probably the fixed step size method (FSSM). We assume that the system is in configuration α at time t, i.e. $\mathcal{P}_\alpha = 1$, and that we want to know the probabilities for some time Δt later. To first order in Δt we have

$$\mathcal{P}_\alpha(t+\Delta t) = 1 - \left[\sum_\beta W_{\beta\alpha}\right]\Delta t \tag{2}$$

and

$$\mathcal{P}_\beta(t+\Delta t) = W_{\beta\alpha}\Delta t, \quad \text{for } \beta \neq \alpha. \tag{3}$$

The MC method now consists of taking a configuration at $t+\Delta t$, that may be the same as the configuration

at t, with the probabilities of Eq. (3). This procedure is repeated for as many time steps Δt as desired. This method, or a variation of it, has been used in most simulations dealing with temperature-programmed reactions (see Ref. [11] and references therein). One drawback of this method, of course, is that Δt must be small as otherwise Eqs. (2) and (3) are no good approximations to the probabilities.

As has been shown by Gillespie [16,17] for reactions in homogeneous systems, and is also known for master equations in general [26,27], it is possible to take one step to each of the subsequent moments that the system changes if the transition probabilities are time-independent. We will show that this is also possible with time-dependent transition probabilities. We define

$$S_\alpha \equiv \sum_\beta W_{\beta\alpha}, \tag{4}$$

and assume that at time $t = 0$ the system is in configuration α. The probability P_α that the system is still in configuration α is given by

$$-\frac{dP_\alpha}{dt} = S_\alpha P_\alpha, \tag{5}$$

with $P_\alpha(0) = 1$. This differential equation has the following formal solution.

$$P_\alpha(t) = \exp\left(-\int_0^t dt' S_\alpha(t')\right). \tag{6}$$

Note the difference between P_α and $\mathcal{P}_\alpha$ of Eq. (1). The former is the probability that no reaction has occurred in α, whereas chains of reactions like $\alpha \rightarrow \beta \rightarrow \alpha$ may contribute to the latter. The probability that the first reaction, which brings the system to another configuration, will occur at time t is given by

$$R_\alpha(t) \equiv -\frac{dP_\alpha}{dt}. \tag{7}$$

We must therefore pick a time for the reaction to occur by generating a random time according to the distribution R_α. We can do this by generating a uniform random number r in the interval $[0, 1]$ and equate this to the probability that the reaction has not yet occurred; i.e.,

$$r = P_\alpha(t). \tag{8}$$

For time-independent transition probabilities this expressions can be solved giving

$$t = -\frac{1}{S_\alpha} \ln r. \tag{9}$$

This expression has been obtained before (see Refs. [26,27]). For reactions on surfaces this method has been used by Nordmeyer and Zaera [18,19]. (Gillespie derives for time-independent transition probabilities first-order expressions for $P_\alpha(\Delta t), P_\alpha(2\Delta t), \ldots, P_\alpha(n\Delta t)$, which become exact in the limit $n \rightarrow \infty$ with $n\Delta t$ = constant [16]. We can do the same for time-dependent transition probabilities. The result is Eq. (6), from which we can derive Eq. (5). We feel, however, that the latter equation is self-evident and have therefore left out this derivation.)

Apart from solving Eq. (8) we also need to determine which reaction takes place. For time-independent transition probabilities we pick a reaction with probability proportional to $W_{\beta\alpha}$. For time-dependent transition probabilities we can do something similar. We define $P_{\beta\alpha}(t)$ as the probability that at time t the reaction leading to configuration β in configuration α has not occurred. We can derive, similar to Eq. (6), the relation

$$P_{\beta\alpha}(t) = \exp\left(-\int_0^t dt' W_{\beta\alpha}(t')\right). \tag{10}$$

We also have the following definition of the probability distribution $R_{\beta\alpha}(t)$ that this reaction will occur at time t.

$$R_{\beta\alpha}(t) \equiv -\frac{dP_{\beta\alpha}}{dt} = W_{\beta\alpha} P_{\beta\alpha}. \tag{11}$$

Now the probability that the reaction to β at time t is the first to occur is given by

$$R_{\beta\alpha}(t) \prod_{\gamma \neq \alpha,\beta} P_{\gamma\alpha}(t) = \frac{R_{\beta\alpha}(t)}{P_{\beta\alpha}(t)} \prod_{\gamma \neq \alpha} P_{\gamma\alpha}(t). \tag{12}$$

From this equation we see that we have to choose the reaction with probability proportional to $R_{\beta\alpha}(t)/P_{\beta\alpha}(t)$. Eq. (11) shows that this ratio is equal to $W_{\beta\alpha}(t)$, where the argument is the time that the first reaction occurs.

This method has the advantages over FSSM that it is exact, and that there is no problem of what to choose

for Δt. The drawback is that one has to be able to solve Eq. (8) efficiently. We will call this method the variable step size method (VSSM).

Gillespie also describes another method he calls the first-reaction method (FRM) [16]. This method too can be generalised to time-dependent transition probabilities. We generate a uniform random number $r_{\beta\alpha}$ in the interval [0, 1] for each possible reaction in configuration α. We define a time $t_{\beta\alpha}$ for each reaction to occur by

$$r_{\beta\alpha} = P_{\beta\alpha}(t_{\beta\alpha}). \tag{13}$$

The reaction that actually happens in α is the one that happens soonest; i.e., the one with the smallest $t_{\beta\alpha}$. This is another method with a variable step size.

This method should be equivalent to VSSM. In the previous method the probability distribution for the time of the first reaction is $R_\alpha(t)$. The probability that the reaction to β is the first to occur and that it occurs at time t is given by Eq. (12). The probability distribution for the time of the first reaction in FRM is than found by summing over all possible reaction; i.e.,

$$\sum_{\beta\neq\alpha} R_{\beta\alpha}(t) \prod_{\gamma\neq\alpha,\beta} P_{\gamma\alpha}(t). \tag{14}$$

From Eqs. (4), (6), and (10) we find immediately

$$P_\alpha(t) = \prod_{\beta\neq\alpha} P_{\beta\alpha}(t). \tag{15}$$

Differentiation gives then

$$R_\alpha(t) = \sum_{\beta\neq\alpha} R_{\beta\alpha}(t) \prod_{\gamma\neq\alpha,\beta} P_{\gamma\alpha}(t), \tag{16}$$

which proves the equivalence of the methods. (It is obvious that the question which reaction occurs first has the same answer in both methods.) According to Gillespie FRM is much less efficient than VSSM, as in FRM Eq. (13) has to be solved for each reaction, whereas for VSSM only one such an equation has to be solved [16]. We will show that for time-dependent transition probabilities the difference between solving Eq. (13) for each reaction and Eq. (8) once is small. Moreover, in case of reactions on a surface Eq. (13) has to be solved at each step for only a small fraction of all reactions. This will make FRM the most efficient method.

In order to determine the efficiency of the three methods, we determine what has to be done in each of the three methods for every time step. We assume that the surface has linear dimension N; i.e., the number of sites in one direction. The number of reactions is then $O(N^2)$. In FSSM all reactions have to be determined, the transition probabilities have to be calculated, a random number has to be generated, and the reaction that actually occurs has to be determined. Except for the generation of the random number, which can be done in $O(1)$ time, this takes in general $O(N^2)$ time.

The determination of all reactions and the determination of the reaction that actually occurs is the same in VSSM as in FSSM. In addition one has to determine the step size which means generating another random number and solving Eq. (8). The additional random number can be done in $O(1)$ time, but solving the equation takes $O(N^2)$ time, because of Eq. (4). In general this is the most time-consuming part of VSSM, but, as the step size is much larger than for an accurate FSSM simulation, VSSM is often much more efficient than FSSM. (We should remark that for FSSM and VSSM there are methods to determine which reaction occurs that are faster than $O(N^2)$ [27,28]. For time-dependent transition probabilities the calculation of these transition probabilities still takes $O(N^2)$ time, so that the method overall is still $O(N^2)$, however.)

For FRM the work is the same as in VSSM, except that a random number has to be generated for each reaction. Solving Eq. (13) for each reaction will take about as much time as solving Eq. (8) once, because the calculation of the transition probabilities is the time-determining step. Generating all random number takes $O(N^2)$ time, but this part is in general negligible compared to solving Eq. (13) itself. One also has to determine the first reaction. This takes $O(N^2)$ time. FRM seems the least efficient method. However, as we will see, the particular type of problem of reactions on a surface offers an opportunity to reduce the work drastically.

One can reduce the work per time step in FRM down to $O(\log N)$ for the present problem. Suppose we have a configuration α and in this configuration a reaction $\alpha \rightarrow \beta$ can occur. However, this reaction does not happen. Instead a reaction $\alpha \rightarrow \alpha'$ occurs. The reactions $\alpha \rightarrow \beta$ and $\alpha \rightarrow \alpha'$ change the configuration in different areas on the surface, or, more precisely, there are no sites that are involved in both reactions. Hence,

in configuration α' we find a reaction $\alpha' \rightarrow \beta'$ that involves the same sites and causes the same changes as $\alpha \rightarrow \beta$. We have defined a reaction as the change of a whole configuration, whereas usually one looks only at the sites that are involved. Therefore, $\alpha \rightarrow \beta$ and $\alpha' \rightarrow \beta'$ are really the same reaction.

We compare the probability distributions for the times that $\alpha \rightarrow \beta$ and $\alpha' \rightarrow \beta'$ occur. If the reaction $\alpha \rightarrow \alpha'$ takes place at time $t = \tau'$ then the probability distribution $R_{\beta'\alpha'}$ for the reaction $\alpha' \rightarrow \beta'$ for $t \geq \tau'$ is given by

$$R_{\beta'\alpha'} = -\frac{\mathrm{d}P_{\beta'\alpha'}}{\mathrm{d}t} = W_{\beta\alpha} P_{\beta'\alpha'}, \tag{17}$$

where $P_{\beta'\alpha'}$ is the probability that the reaction has not occurred, with boundary condition $P_{\beta'\alpha'}(\tau') = 1$. Note that $W_{\beta'\alpha'} = W_{\beta\alpha}$, because $\alpha \rightarrow \beta$ and $\alpha' \rightarrow \beta'$ are really the same reaction. For the reaction $\alpha \rightarrow \beta$ we have

$$R_{\beta\alpha} = -\frac{\mathrm{d}P_{\beta\alpha}}{\mathrm{d}t} = W_{\beta\alpha} P_{\beta\alpha}, \tag{18}$$

with $P_{\beta\alpha}(\tau) = 1$, where τ is the time we start with configuration α. As Eqs. (17) and (18) are linear, we find immediately that for $t \geq \tau'$ $P_{\beta'\alpha'}$ is proportional to $P_{\beta\alpha}$, and hence that $R_{\beta'\alpha'}$ is proportional to $R_{\beta\alpha}$. Thus the relative probability for generating a reaction time for $\alpha \rightarrow \beta$ and $\alpha' \rightarrow \beta'$ is the same for $t \geq \tau'$. This means that it is not necessary to generate a time for $\alpha' \rightarrow \beta'$, but we can use the time for $\alpha \rightarrow \beta$ that we already have.

The only reactions for which new times have to be generated are the ones that have only just become possible, because of the changes due to $\alpha \rightarrow \alpha'$. The number of these reactions does not depend on the size N of the surface, as a reaction changes the surface only locally. Consequently, the only work that needs to be done in FRM and that depends on N has to do with getting the first reaction. It is most convenient to retain a time-ordered list of all possible reactions. The new reactions have to be inserted in this time-ordered list and the first reaction has to be retrieved, which can be done in $O(\log N)$ time. Note that those reactions that are no longer possible after $\alpha \rightarrow \alpha'$ should not be removed from the list, as scanning the whole list would take $O(N^2)$ time. Instead one should test if a reaction is still possible before changing the configuration. The time-ordered list of reactions will contain a (large) fraction of impossible reactions. This fraction, however, will not depend on N.

2.3. Generating reaction times

In this subsection we show how to solve Eq. (13). This will depend on the form we have for $P_{\beta\alpha}$, which in term depends on $W_{\beta\alpha}$ in Eq. (11). We have already more or less seen one solution for Eq. (11), namely the solution for the case of a time-independent transition probability, which is

$$P_{\beta\alpha} = \exp(-W_{\beta\alpha} t), \tag{19}$$

which yields for Eq. (13)

$$t_{\beta\alpha} = -\frac{1}{W_{\beta\alpha}} \ln r_{\beta\alpha}. \tag{20}$$

Here we are interested in the case where we can write

$$W = \nu_0 \exp\left(-\frac{E_{\mathrm{act}}}{k_{\mathrm{B}} T}\right), \tag{21}$$

where E_{act} is the activation energy, ν_0 is the pre-exponential factor, k_{B} is the Boltzmann constant, and T is the temperature. We have dropped the configuration indices for convenience. The activation energy and the pre-exponential factor we will assume constant. The time dependence will enter only through the time dependence of the temperature. For temperature-programmed reaction experiments we usually have

$$T = T_0 + Bt, \tag{22}$$

where T_0 and B are constants. We will deal with this time dependence only.

As can be seen from Eq. (10) we need to be able to calculate the integral $\int_0^t \mathrm{d}t' W(t')$. With Eqs. (21) and (22) this is possible. The result is

$$\int_0^t \mathrm{d}t' W(t') = \Omega(t) - \Omega(0), \tag{23}$$

where

$$\Omega(t) = \frac{\nu_0}{B}(T_0 + Bt) E_2\left(\frac{E_{\mathrm{act}}}{k_{\mathrm{B}}(T_0 + Bt)}\right), \tag{24}$$

and where E_2 is an exponential integral [29].

We have not been able to find this analytical expression for the solution of Eq. (13) in the literature. As

an aside we would like to show another application of Eq. (23). Consider desorption of order n, which is described by

$$\frac{d\theta}{dt} = -k\theta^n, \tag{25}$$

where θ is the coverage, n is some non-negative integer, and k is given by an expression like Eq. (21). For a temperature-programmed desorption experiment with Eq. (22) holding, we have for zero-order desorption

$$\theta(t) = \theta_i - [\Omega(t) - \Omega(0)], \tag{26}$$

where θ_i is the coverage at $t = 0$. From

$$\frac{d\Omega}{dt} = \nu_0 \exp\left(-\frac{E_{act}}{k_B T}\right) > 0, \tag{27}$$

we see that $\Omega(t)$ is monotone increasing. ($E_{act}, \nu_0 > 0$.) Moreover, the derivative is also monotone increasing. Hence, $\theta(t) \to -\infty$ for strict zero-order desorption. In fact, this shows that Eq. (25) cannot describe a zero-order temperature-programmed desorption spectrum completely, but only the left flank of a zero-order peak.

For first-order desorption we find

$$\theta(t) = \theta_i \exp\{-[\Omega(t) - \Omega(0)]\}. \tag{28}$$

This is essentially what we will see below for the expression of the reaction time. For second- and higher-order desorption we find

$$\theta(t) = \frac{\theta_i}{\{1 - \theta_i^{n-1}[\Omega(t) - \Omega(0)]\}^{1/(n-1)}}. \tag{29}$$

Eqs. (26), (28), and (29) may be used to fit TPD spectra, and thus obtain estimates for the activation energy and the pre-exponential factor from the whole TPD spectrum. Current methods use only information like peak maximum temperature and peak width [2]. Similar expressions might also be derived for other types of reactions.

Using Eqs. (10) and (23) we can rewrite Eq. (13) as

$$r = \exp\{-[\Omega(t) - \Omega(0)]\}. \tag{30}$$

We know of no analytical solution for this equation. However, using the properties of $\Omega(t)$, an efficient and robust numerical method is possible. We rewrite the last equation as

$$\Omega(t) = \Omega(0) - \ln r. \tag{31}$$

This equation can be solved most conveniently with the Newton-Raphson method [30]. As Ω and $d\Omega/dt$ are both monotone increasing, the method always succeeds, the derivative of Ω is simple, and the convergence is fast.

3. Examples

In this section we present four examples. The purpose of these examples is a demonstration of various aspects of the method presented in the previous section, rather than to present new results. In all examples we have used a square grid and periodic boundary conditions. All simulations have been done with our code PIZZAZZ[2].

3.1. Desorption without lateral interactions

The simplest case deals with temperature-programmed desorption of atoms without lateral interactions. This corresponds to first-order desorption, which allows us to compare the results of the simulation with exact results. We derive a macroscopic reaction-rate equation from the master equation. With A the number of atoms on the surface and S the number of sites, we have

$$\theta \equiv \frac{\langle A \rangle}{S} \equiv \frac{1}{S}\sum_\alpha \mathcal{P}_\alpha A_\alpha, \tag{32}$$

where θ is the coverage and A_α is the number of atoms in configuration α. Using Eq. (1) we get

$$\begin{aligned}\frac{d\theta}{dt} &= \frac{1}{S}\sum_\alpha \frac{d\mathcal{P}_\alpha}{dt} A_\alpha \\ &= \frac{1}{S}\sum_{\alpha\beta}[W_{\alpha\beta}\mathcal{P}_\beta - W_{\beta\alpha}\mathcal{P}_\alpha]A_\alpha \\ &= \frac{1}{S}\sum_{\alpha\beta} W_{\alpha\beta}\mathcal{P}_\beta[A_\alpha - A_\beta].\end{aligned} \tag{33}$$

[2] PIZZAZZ is a general-purpose program, written in C++, for simulating reactions on surfaces that can be represented by regular grids. It is an implementation of the first-reaction method.

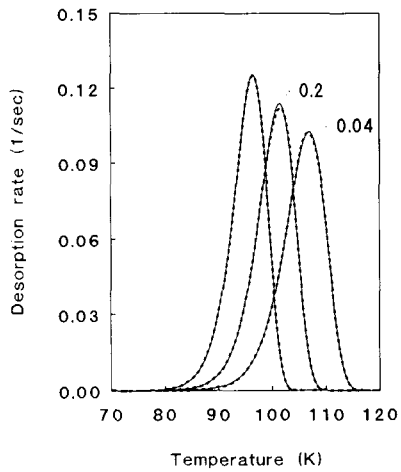

Fig. 1. TPD spectra (desorption rate per site (in s^{-1}) as a function of temperature (in K)) of desorption without lateral interactions with transition probabilities given by Eq. (21), $E_{act}/k_B = 3000\,K$, and $\nu_0 = 10^{13}\,s^{-1}$. The dashed curves are averaged results of ten MC simulations on a 100×100 square grid. The solid curves are solutions of the corresponding macroscopic reaction-rate equation Eq. (34). Spectra are shown, peaks from left to right, for heating rates 1, 5, and $25\,K\,s^{-1}$, respectively, and monolayer initial coverage. The peaks for 5 and $25\,K\,s^{-1}$ are scaled down by the factors shown.

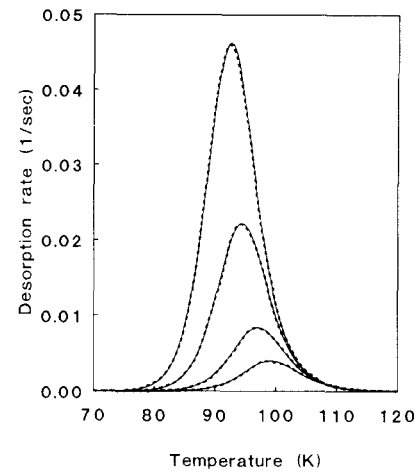

Fig. 2. TPD spectra (desorption rate per site (in s^{-1}) as a function of temperature (in K)) of associative desorption with transition probabilities given by Eq. (21), $E_{act}/k_B = 3000\,K$, and $\nu_0 = 10^{13}\,s^{-1}$ for the desorption, and $E_{act}/k_B = 3000\,K$, and $\nu_0 = 5 \times 10^{13}\,s^{-1}$ for the diffusion. The dashed curves are averaged results of 20 MC simulations on a 100×100 square grid. The solid curves are solutions of the corresponding macroscopic reaction-rate equation Eq. (35). Spectra are shown for initial coverage 1.0, 0.5, 0.2, and 0.1, and the heating rate is $1\,K\,s^{-1}$.

The double summation in this expression contributes only if $A_\alpha = A_\beta - 1$. There are A_β of such terms for each configuration β. If we put $W_{\alpha\beta} = k_1$ for each of these, we get

$$\frac{d\theta}{dt} = -\frac{k_1}{S}\sum_\beta A_\beta \mathcal{P}_\beta = -k_1\theta. \tag{34}$$

This is the desired macroscopic equation.

In Fig. 1 we show the desorption rate $-d\theta/dt$ obtained from a simulation and by solving Eq. (34) exactly (see Eq. (28)). We see an excellent agreement. The activation energy and the pre-exponential factor are more or less those for Xe desorption form Pt(111) [31].

3.2. Associative desorption

We can also compare the results for associative desorption $2A(ads) \rightarrow A_2(gas)$ with exact ones. We find again Eq. (33), but now $A_\alpha = A_\beta - 2$. This does not suffice to do the summations. We therefore make the assumption that the atoms are randomly distributed over the sites. The number of terms that contributes in Eq. (33) equals the number of A–A nearest-neighbour pairs. This equals the number of pairs of nearest neighbour sites $SZ/2$, where Z is the number of neighbouring sites, times the probability that both sites are occupied $(A_\beta/S)^2$. If we put $W_{\alpha\beta} = k_2$ for each contributing term we find

$$\frac{d\theta}{dt} = -\frac{k_2 Z}{S^2}\langle A^2\rangle = -k_2 Z\theta^2 - k_2 Z\frac{(\Delta A)^2}{S^2}, \tag{35}$$

where ΔA is the fluctuation in the number of atoms on the surface. This scales as $\Delta A \propto \sqrt{S}$, so that in the thermodynamic limit the last term vanishes. (This can be proven more rigorously using the method in Chapter IX of Ref. [21].)

Fig. 2 shows results of a simulation compared with exact solutions (see also Eq. (29)). Again the agreement is excellent. In order to get a random distribution of the atoms in the simulation the atoms must be allowed to diffuse over the surface. Moreover, the diffusion must be fast compared to the desorption. Using smaller transition probabilities for the diffusion than in Fig. 2 results in lower peaks with longer tails. However, the effect is small as long as the diffusion is not slower than the desorption, especially when having

high initial coverages. The fluctuation term in Eq. (35) for finite surfaces does not seem to be important. No effect whatsoever was found for grid sizes as small as 10×10.

3.3. Desorption with lateral interactions

Repulsive lateral interactions are known to yield spectra with multiple peaks at high initial coverages. We have simulated monoatomic desorption using parameter set F of Meng and Weinberg [32] (all prefactors for desorption $10^{13}\,s^{-1}$, and activation energy $(15398 - 1006N_{nn})$ K, where N_{nn} is the number of nearest neighbours). We used the same activation energies for diffusion (the number of nearest neighbours were counted before a jump was made to another site), but various prefactors were tested. The ratio between the transition probabilities of diffusion and desorption was temperature independent. We found no changes in the TPD spectra for a diffusion prefactor five (i.e., $5 \times 10^{13}\,s^{-1}$) or more times the desorption prefactor. This should correspond to the thermal equilibrium on the surface in the method of Meng and Weinberg.

Fig. 3 shows desorption spectra for various initial coverages. The results agree well with those of Meng and Weinberg [32], except that the high-temperature peak is at a somewhat lower temperature, and it is somewhat smaller. An analysis, as described below, shows that this is caused by a relatively large contribution from desorbing atoms having one, two, or three nearest neighbours (atoms with four nearest neighbours contribute only to the low-temperature peak). Decreasing the prefactor of the transition probability for the diffusion down to about $10^{12}\,s^{-1}$ does give a position and height for the high-temperature peak as found by Meng and Weinberg. This suggests that no equilibrium was reached in the simulations of Meng and Weinberg.

It is very instructive to decompose the peaks into contributions of desorbing atoms with a particular number of nearest neighbours. As is shown in Fig. 4 the low-temperature peak is caused exclusively by atoms with four nearest neighbours. The high-temperature peak is caused by atoms with none, one, two, or three nearest neighbours. The contribution to this peak of atoms with one or more nearest neighbours is surprisingly large. The reason is that, even though there are far fewer atoms with than there

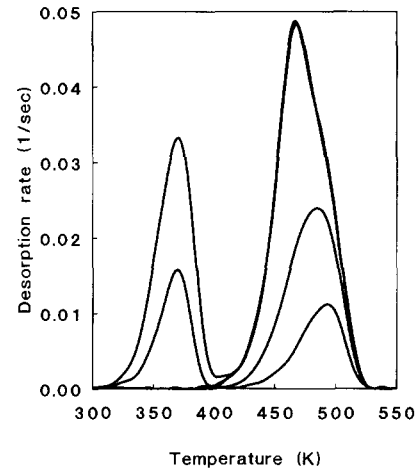

Fig. 3. TPD spectra (desorption rate per site (in s^{-1}) as a function of temperature (in K)) of desorbing atoms with lateral interaction described by parameter set F of Ref. [32]. The curves are averaged results of 25 MC simulations on a 60×60 square grid. Spectra are shown for initial coverage 0.7, 0.6, 0.5, 0.2, and 0.1, and the heating rate is $5\,K\,s^{-1}$. The spectra for initial coverages 0.7 and 0.6 consist of a low- and a high-temperature peak. The spectra of 0.5, 0.2, and 0.1 only show a high-temperature peak. At high temperature the curves for initial coverages 0.7, 0.6, and 0.5 coincide.

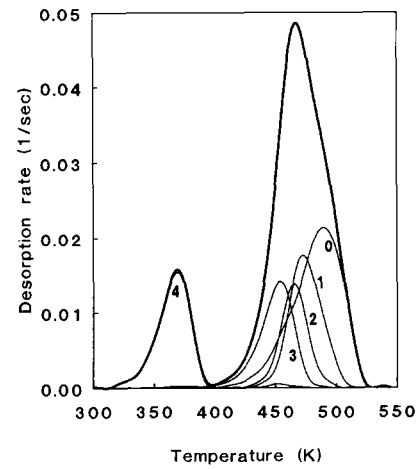

Fig. 4. Decomposition of TPD spectrum from Fig. 3 with initial coverage 0.6. The fat curve is the TPD spectrum, and the thinner curves are contributions, from right to left, from atoms desorbing when having no, one, two, three, and four nearest neighbours. The curve for four nearest neighbours almost coincides with the TPD low-temperature peak.

are without nearest neighbours, this may be more than compensated for by a large desorption probability. Another consequence is that for initial coverage below half a monolayer the high-temperature peak shifts to higher temperature with decreasing initial coverage, because the contribution from atoms with nearest neighbours decreases. This is not to be expected when the high-temperature peak is caused by (first-order) desorption of atoms without nearest neighbours. Decreasing the initial coverage from one to half a monolayer only caused a scaling down of the low-temperature peak.

3.4. Desorption with dissociation and recombination

As a final example we simulate the following TPD-experiment. A diatomic molecule A_2 is adsorbed at low temperature. Three reactions are possible.

$$A_2(\text{ads}) \rightarrow 2A(\text{ads}), \tag{36}$$

$$2A(\text{ads}) \rightarrow A_2(\text{ads}), \tag{37}$$

$$A_2(\text{ads}) \rightarrow A_2(\text{gas}). \tag{38}$$

The transition probabilities are given by Eq. (21) with $E_{\text{act}}/k_B = 5000\,\text{K}$, $\nu_0 = 10^7\,\text{s}^{-1}$ for the dissociation, $E_{\text{act}}/k_B = 13000\,\text{K}$, $\nu_0 = 10^{10}\,\text{s}^{-1}$ for the recombination, and $E_{\text{act}}/k_B = 13000\,\text{K}$, $\nu_0 = 10^{16}\,\text{s}^{-1}$ for the desorption. There is no diffusion. This model (and to a certain extent also the parameters) is chosen to resemble a TPD-experiment of the reduction of NO on Rh(111) [33]. Of course, no difference is made between nitrogen and oxygen and a square grid is used.

The TPD-spectra of A_2 desorption are shown in Fig. 5. We see that at high coverage there are two peaks, whereas there is only one at low coverage. The low-temperature peak is clearly a first-order desorption peak. Indeed, without the dissociation and recombination reaction we would have only this low-temperature peak. At low coverage the molecule dissociates before it desorbes. At high temperature the recombination becomes possible, which is immediately followed by a desorption. The high-temperature peak seems second-order, because of the recombination reaction. The reason why there is a low-temperature peak at high coverage is that some molecules cannot dissociate, because their neighbouring sites are already occupied by A_2 or A.

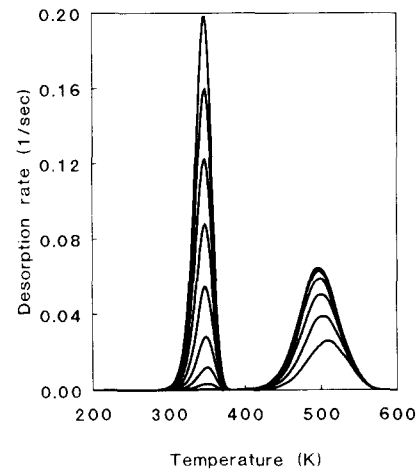

Fig. 5. TPD spectra (desorption rate per site (in s^{-1}) as a function of temperature (in K)) of A_2 desorption for the system described in Section 3.4. The curves are averaged results of 16 MC simulations on a 80×80 square grid. Spectra are shown for initial coverage 0.2, 0.3, . . ., 1.0, and the heating rate is $10\,\text{K}\,\text{s}^{-1}$. At low temperature there is no desorption for initial coverage 0.2. At high temperature the curves for initial coverages 0.6, 0.7, 0.8, 0.9, and 1.0 coincide.

Fig. 6 shows the rate of the dissociation. At low coverage we have only one peak. At high coverage we have two peaks, because of the blocking of neighbouring sites just mentioned. Some molecules can only dissociate after sites become unoccupied, because other molecules start desorbing. An extreme case is where we start with monolayer coverage; the low-temperature peak has completely disappeared, as no molecule can dissociate until others desorb. Because of the blocking effect there can be two reactions with very different rates (see Fig. 7) at the same time. If the initial coverage is high then dissociation stops when all remaining A_2 molecules cannot dissociate, because of blocked neighbouring sites. When desorption of an A_2 molecule occurs that has another A_2 molecule as nearest neighbour, the desorption is immediately followed by a dissociation. At high temperature recombination and desorption alternate, as each recombination reaction is immediately followed by the desorption of the A_2 molecule that is formed.

3.5. Timings

Although the computational time that is used by a simulation varies depending on many factors, we think

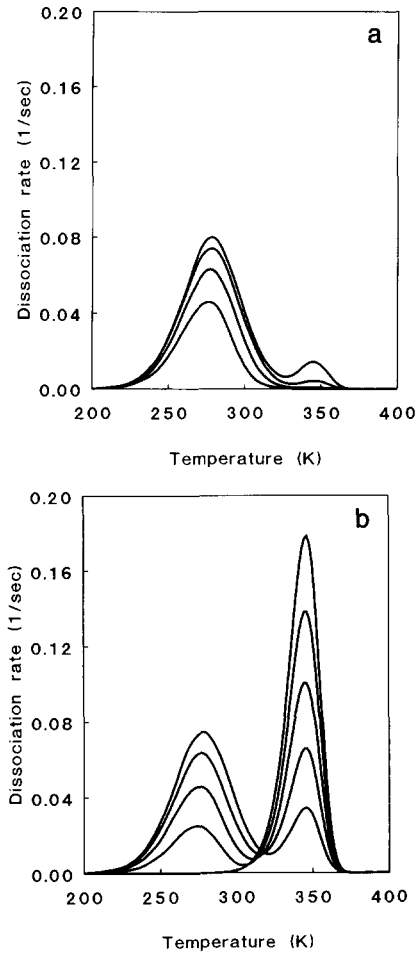

Fig. 6. Reaction rate per site (in s^{-1}) for the dissociation Eq. (36) as a function of temperature (in K). The curves are averaged results of 16 MC simulations on a 80×80 square grid. Initial coverages are 0.2, 0.3, 0.4, and 0.5 (a), and 0.6, 0.7, 0.8, 0.9, and 1.0 (b). The heating rate is $10\,K\,s^{-1}$. In (b) higher initial coverages yield higher peaks at high temperature, but lower peaks at low temperature. There is no low-temperature peak for initial coverage 1.0.

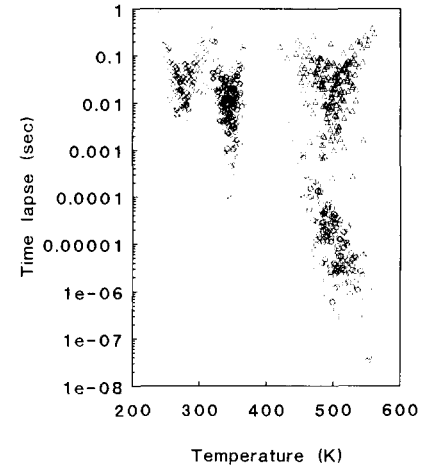

Fig. 7. Each symbol stands for a reaction. On the horizontal axis is the temperature (in K) at which the reaction occurred. On the vertical axis is the time (in s) that has lapsed since the preceding reaction. Shown are the results for a typical MC simulation of the system of Section 3.4 on a 25×25 square grid with initial coverage 0.7 and heating rate $10\,K\,s^{-1}$. The dissociation is depicted by diamonds, the recombination by triangles, and the desorption by circles.

Table 1
Computational time per reaction that actually occurred given by $a_0 + a_1 \log N$

Example	a_0 (s)	a_1 (s)	fraction
Section 3.1	1.6×10^{-5}	2.0×10^{-5}	1.00
Section 3.2	8.7×10^{-5}	1.1×10^{-4}	≈ 0.23
Section 3.3	1.6×10^{-3}	2.1×10^{-4}	≈ 0.10
Section 3.4	4.4×10^{-4}	9.9×10^{-5}	≈ 0.19

The rightmost column shows the fraction of all reactions that were found, that actually occurred. The initial coverage in all cases was $\theta_i = 1$, except for the example of Section 3.3 where $\theta_i = 0.6$.

that it is nevertheless useful to get an impression of the costs of the simulations of the previous subsections. All simulations were done on a Silicon Graphics Iris Indigo with one R4400 processor using the PIZZAZZ code. Table 1 shows the computational time per reaction that actually occurred. The timings confirm the analysis in Section 2.2 that the simulations take $O(\log N)$ time, where N is the linear dimension of the surface; i.e., the number of sites in one direction. Table 1 was obtained using $N = 10, 20, 40, \ldots, 640$. We see that the N independent part is about the same order of magnitude as the $\log N$ dependent part. This implies that FRM is much more efficient than VSSM (of FSSM). In FRM the calculation of the reaction times contributes to the N independent part as only reaction times for new reactions have to be determined; i.e., solving Eq. (13) has only to be done an N independent small number of times. In VSSM Eq. (8) has only to be solved once per time step, but this takes $O(N^2)$ times solving Eq. (13).

The $\log N$ dependence of FRM results from inserting and retrieving reactions in the time-ordered list of all reactions. It may be a bit surprising that the coefficient of $\log N$ differs so much for the four examples,

Table 2
Computational time per reaction that was found given by $a_0 + a_1 \log N$

Example	a_0 (s)	a_1 (s)
Section 3.1	1.6×10^{-5}	2.0×10^{-5}
Section 3.2	2.0×10^{-5}	2.6×10^{-5}
Section 3.3	1.4×10^{-4}	2.5×10^{-5}
Section 3.4	8.4×10^{-5}	1.9×10^{-5}

The initial coverage in all cases was $\theta_i = 1$, except for the example of Section 3.3 where $\theta_i = 0.6$.

but this is because not every reaction that is found during the simulation also actually occurs. The last column of Table 1 shows the fraction of all reactions that are found and have also occurred. Table 2 shows the computational time per reaction that is found sometime during the simulation. We see that the coefficients of $\log N$ are now much more similar. We think that the differences arise mainly because the binary search tree that is used for storing the reaction is not always optimal. The N dependent part in Table 2 is more or less proportional to the number of new reactions that are found on average each time step.

We have also compared solving Eq. (13) via Eq. (31) with using Eq. (20) for the example of Section 3.1. We found that Eq. (31) was only a factor six slower than Eq. (20) when the reaction time was determined with a accuracy of 10^{-6} K.

4. Conclusions

We have generalised Gillespie's Monte Carlo methods for simulating chemical reactions. The methods in this paper can also be used for heterogeneous systems and for time-dependent reaction-rate constants. More specifically, we have looked at simulations of temperature-programmed desorption experiments, and explicit expressions have been derived for the case where temperature varies linearly with time. When reactions change the configuration of the adsorbates on a surface only locally, the first-reaction method is most efficient as the computational time per reaction scales only with the logarithm of the size of the surface in the simulation. Examples have shown that the method is also very accurate, and that it can handle simultaneously reactions with very different reaction rates.

Acknowledgements

I would like to thank Prof. R.A. van Santen for suggesting the subject of this paper, and Dr. M. Neurock and Prof. P.A.J. Hilbers for their stimulating discussions.

References

[1] D. Menzel, in: Chemistry and Physics of Solid Surfaces IV, eds. R. Vanselow and R. Howe (Springer, Berlin, 1982) p. 389.
[2] J.T. Yates, in: Methods of Experimental Physics, Vol. 22, eds. R.L. Park and M.G. Lagally (Academic, Orlando, 1985) p. 425.
[3] J.L. Sales and G. Zgrablich, Phys. Rev. B35 (1987) 9520.
[4] E.S. Hood, B.H. Toby, and W.H. Weinberg, Phys. Rev. Lett. 55 (1985) 2437.
[5] D. Gupta and C.S. Hirzel, Chem. Phys. Lett. 149 (1988) 527.
[6] D. Gupta and C.S. Hirzel, Surf. Sci. 210 (1989) 322.
[7] S.J. Lombardo and A.T. Bell, Surf. Sci. 206 (1988) 101.
[8] S.J. Lombardo and A.T. Bell, Surf. Sci. 224 (1989) 451.
[9] M. Silverberg, A. Bin-Shaul, and F. Rebentrost, J. Chem. Phys. 83 (1985) 6501.
[10] M. Silverberg, A. Bin-Shaul, and F. Rebentrost, J. Chem. Phys. 87 (1987) 3178.
[11] S.J. Lombardo and A.T. Bell, Surf. Sci. Rep. 13 (1991) 1.
[12] H.C. Kang and W.H. Weinberg, Surf. Sci. 299/300 (1994) 755.
[13] R.M. Ziff, E. Gulari, and Y. Barshad, Phys. Rev. Lett. 56 (1986) 2553.
[14] P. Gray and S.K. Scott, Chemical Oscillations and Instabilities: Non-Linear Chemical Kinetics (Clarendon, Oxford, 1990).
[15] R. Imbihl, A.E. Reynolds, and D. Kaletta, Phys. Rev. Lett. 67 (1991) 275.
[16] D.T. Gillespie, J. Comp. Phys. 22 (1976) 403.
[17] D.T. Gillespie, J. Phys. Chem. 81 (1977) 2340.
[18] T. Nordmeyer and F. Zaera, Chem. Phys. Lett. 183 (1991) 195.
[19] T. Nordmeyer and F. Zaera, J. Chem. Phys. 97 (1992) 9345.
[20] Y.S. Matros, Chem. Eng. Sci. 45 (1990) 2097.
[21] N.G. van Kampen, Stochastic Processes in Physics and Chemistry (North-Holland, Amsterdam, 1981).
[22] J.C. Keck, Adv. Chem. Phys. 13 (1967) 85.
[23] H. Burghgraef, A.P.J. Jansen, and R.A. van Santen, Chem. Phys. 177 (1993) 407.
[24] H. Burghgraef, A.P.J. Jansen, and R.A. van Santen, Faraday Discuss. Chem. Soc. 96 (1993) 337.
[25] S.R. Blaszkowski, A.P.J. Jansen, M.A.C. Nascimento, and R.A. van Santen, submitted to J. Phys. Chem..
[26] K. Binder, in: Monte Carlo Methods in Statistical Physics, Topics in Current Physics, Vol. 7, ed. K. Binder, (Springer, Berlin, 1986) p. 1.

[27] J. Honerkamp, Stochastische Dynamische Systeme (VCH, Weinheim, 1990).
[28] T. Fricke and J. Schnakenberg, Z. Phys. B–Condensed Matter 83 (1991) 277.
[29] M. Abramowitz and I.A. Stegun, Handbook of Mathematical Functions (Dover, New York, 1970).
[30] W.H. Press, B.P. Flannery, S.A. Teukolshy, and W.T. Vetterling, Numerical Recipes in C (Cambridge, Cambridge, 1992).
[31] A.P.J. Jansen, J. Chem. Phys. 97 (1992) 5205.
[32] B. Meng and W.H. Weinberg, J. Chem. Phys. 100 (1994) 5280.
[33] H.J. Borg, J.F.C.-J.M. Reijerse, R.A. van Santen, and J.W. Niemantsverdriet, To appear in J. Chem. Phys. 101 (1994).